JOURNAL OF Materials CHEMISTRY

N-Alkyl-*p*-nitroanilines: impact of alkyl chain length on crystal structures and optical SHG

P. Gangopadhyay,[a] S. Venugopal Rao,[b] D. Narayana Rao[b] and T. P. Radhakrishnan*[a]

[a]*School of Chemistry and* [b]*School of Physics, University of Hyderabad, Hyderabad 500 046, India. E-mail: tprsc@uohyd.ernet.in; Fax: 91-40-3010120, 3010145*

Received 1st March 1999, Accepted 4th May 1999

N-Alkyl-*p*-nitroanilines from the propyl to the octyl derivative are synthesised and characterised. Powder SHG studies show that the butyl derivative alone is active, in agreement with earlier observations. Crystal structures of the propyl, butyl and pentyl derivatives are determined; the propyl and pentyl derivatives belong to the centrosymmetric space groups $P\bar{1}$ and $P2_1/c$ respectively and the butyl derivative to the noncentrosymmetric $P2_12_12_1$ space group. Detailed analysis of these structures provides insight into the critical role of the alkyl chain length in the formation of centrosymmetric or noncentrosymmetric crystal lattices. The utility of alkyl chain length as a crystal design element for quadratic NLO materials is noted.

Introduction

Molecules possessing electron donating and accepting groups connected by extended π-electron pathways generally possess large hyperpolarisabilities, β. Noncentrosymmetric assemblies of such molecules in the form of single crystals and thin films with appropriate alignment of the β tensor components display efficient quadratic nonlinear optical (NLO) properties.[1] One of the most popular NLO applications sought in such materials is optical second harmonic generation (SHG). In the two stage fabrication of molecular materials for SHG involving the synthesis of the molecular unit followed by the assembly of the noncentrosymmetric bulk material, the latter is the more difficult step and a variety of chemical and physical routes have been explored for this purpose. The chemical approaches based on the modification of molecular structures exploit features such as intermolecular H-bonding,[2] steric factors,[3] vanishing ground state dipole moments,[4] molecular chirality[5] and salt formation.[6] The physical techniques used to obtain acentric structures include electric field poling in thin films,[7] formation of X and Z type Langmuir–Blodgett films[8] and formation of host–guest systems.[9] Though lack of a centre of inversion is a necessary prerequisite, suitable alignment of the molecules is required to obtain efficient SHG active materials.[10] Development of novel molecular and crystal design techniques for assembling such materials is of great current interest.

p-Nitroaniline (pNA) is the prototypical push–pull conjugated molecule with appreciable hyperpolarisability of potential interest in NLO applications. Since pNA itself has a centrosymmetric crystal lattice,[11] several related molecules have been investigated for SHG capability in the crystalline form. The simplest successful modifications include *m*-nitroaniline (mNA)[12] and 2-methyl-4-nitroaniline (MNA),[3a,3b,13] both of which have noncentrosymmetric crystal lattices and show powder SHG of 20 and 80 U respectively (1 U = SHG of urea). The chiral derivative 2,4-dinitrophenyl-(L)-alanine methyl ester (MAP)[14] shows a moderate SHG of 10 U. *N*-4-Nitrophenyl-(*S*)-prolinol (NPP)[15] is a derivative designed to exploit intermolecular H-bonding interactions and molecular chirality simultaneously and has a near optimal orientation of the dipoles in the crystal lattice leading to a high SHG capability of 150 U. The λ-shaped packing motif in 4-nitrophenylhydrazones leads to noncentrosymmetric materials capable of very strong SHG.[16] A good sampling of the large number of pNA derivatives that are SHG active may be found in Ref. 17. pNA itself has been incorporated in a variety of host lattices so that the antiparallel alignment of the molecular dipoles present in the native crystal lattice is broken and SHG activity is achieved. Moderate SHG has been observed in pNA incorporated in poly(methyl methacrylate) film[18] as well as in pNA included to optimum levels in molecular sieves.[19] An intercalation compound of pNA in tetramethylammonium saponite prepared in the presence of an electric field showed great enhancement of SHG activity over the compound prepared in the absence of the electric field.[20]

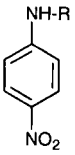

R =	*n*-propyl	**1**
	n-butyl	**2**
	n-pentyl	**3**
	n-hexyl	**4**
	n-heptyl	**5**
	n-octyl	**6**

Another interesting approach reported for the induction of SHG activity in pNA derivatives involves the introduction of an *n*-alkyl chain on the amino group of pNA.[21] Powder SHG studies were carried out on *N*-propyl, *N*-butyl, *N*-pentyl, *N*-hexyl and *N*-octyl derivatives of pNA. Though the linear optical properties of these compounds were very similar, only the *N*-butyl derivative showed SHG activity. Crystal structures of these derivatives have not been reported so far and the origin of this interesting phenomenon has not been investigated. Among the simple *n*-alkyl derivatives of pNA, structural studies have been published only on three systems: the *N*-methyl[22] and *N*,*N*-diethyl[23] derivatives form centrosymmetric crystals belonging to the $P2_1/n$ space group and the *N*,*N*-dimethyl[24] derivative has an acentric structure ($P2_1$) resulting in moderate SHG capability. An interesting observation of SHG activity in powder mixtures of pNA with *N*-alkylated pNA has also been reported.[25] However, since these studies were carried out on powders, no structural characterisations are available to explain the observed NLO properties. We have recently discovered chain length dependent SHG activity in *n*-alkyl substituted diaminodicyanoquinodimethanes[26] in a manner similar to that observed in *n*-alkyl substituted pNA's. The potential utility of alkyl chain length as a crystal design element for fabricating noncentrosymmetric crystal lattices of interest in quadratic NLO applications prompted us to carry out detailed structural investigations on the pNA derivatives. The varying powder SHG reported[21,25] for *N*-alkyl pNA's recrystallised under different conditions points to the possibility of polymorphism. We have synthesised and characterised the *N*-propyl (**1**), *N*-butyl (**2**), *N*-pentyl (**3**), *N*-hexyl (**4**), *N*-heptyl (**5**) and *N*-octyl (**6**) derivatives of pNA. We have also

carried out a systematic investigation of these compounds by recrystallising all of them from the same solvent system and examining the crystal structures of three derivatives **1**, **2** and **3**. We present a detailed analysis of the crucial role of the alkyl chain in steering the crystal packing which effectively controls the optical SHG capability of these materials.

Experimental

Synthesis and characterisation

All the compounds were synthesised following the procedure reported in Ref. 27. The detailed procedure is illustrated using the case of **2** as an example. 1.000 g (0.8 ml, 7.0 mmol) of 4-fluoronitrobenzene was dissolved in 8 ml of freshly dried and distilled DMSO and stirred at 75 °C. 2.8 g (20 mmol) of freshly ignited and subsequently cooled potassium bicarbonate was added to the solution and stirred. 1.243 g (1.7 ml, 17 mmol) of dry *n*-butylamine was added to the mixture and refluxed at 120 °C under dry nitrogen gas. The progress of the reaction was monitored by TLC; about 98% conversion was observed after 6 h. The reaction mixture was cooled and poured over 200 g of crushed ice and stirred vigorously for 30 min. The yellow precipitate formed was filtered and washed with water thoroughly. The filter cake was dried in air to give 1.3 g (96% yield) of **2**. It was purified by eluting through a basic alumina column using ethyl acetate–hexane (65:35) mixture. Further purification was carried out by sublimation at 80 °C under reduced pressure. Crystals were grown from toluene–chloroform (70:30) mixture. **1**, **3**, **4**, **5** and **6** were synthesised similarly and recrystallised using the same solvents. The yields for the various compounds were 85 to 96%.

***N*-Propyl-4-nitroaniline (1).** Mp: 72 °C; UV–Vis (methanol): $\lambda_{max}=387$ nm, $\lambda_{cut\text{-}off}=490$ nm; FT-IR (KBr pellet): $\bar{\nu}/cm^{-1}=3346.8$ (N–H stretch), 2957.1, 2926.0 (aliphatic C–H stretch), 2817.2 (CH_2: C–H stretch), 1473.8, 1300.0 (NO_2 stretches); E. I. mass: $m/z=180$ (M^+), 151, 105; ^{1}H-NMR ($CDCl_3$, δ from TMS): 1.03 (t, 3H), 1.64–1.75 (m, 2H), 3.19 (q, 2H), 4.50 (broad, 1H), 6.52 (q, 2H), 8.08 (q, 2H); ^{13}C-NMR ($CDCl_3$, ppm): 11.40, 22.42, 45.20, 110.92, 126.39, 153.45; elemental analysis (calculated for $C_9H_{12}N_2O_2$): %C = 59.93 (59.99), %H = 6.76 (6.71), %N = 15.52 (15.55).

***N*-Butyl-4-nitroaniline (2).** Mp: 68–70 °C; UV–Vis (methanol): $\lambda_{max}=386$ nm; $\lambda_{cut\text{-}off}=487$ nm; FT-IR (KBr pellet): $\bar{\nu}/cm^{-1}=3339.1$ (N–H stretch), 2959.1, 2926.3 (aliphatic C–H stretch), 2817.2 (CH_2: C–H stretch), 1462.2, 1319.4 (NO_2 stretches); E. I. mass: $m/z=194$ (M^+), 151, 105; ^{1}H-NMR ($CDCl_3$, δ from TMS): 1.01 (t, 3H), 1.39–1.46 (m, 2H), 1.50–1.69 (m, 2H), 3.16–3.26 (q, 2H), 4.5 (broad, 1H), 6.51 (d, 2H), 8.08 (d, 2H); ^{13}C-NMR ($CDCl_3$, ppm): 13.71, 20.13, 31.23, 43.14, 110.91, 126.41, 153.50; elemental analysis (calculated for $C_{10}H_{14}N_2O_2$): %C = 61.37 (61.84), %H = 7.28 (7.27), %N = 14.49 (14.42).

***N*-Pentyl-4-nitroaniline (3).** Mp: 67–68 °C; UV–Vis (methanol): $\lambda_{max}=386$ nm, $\lambda_{cut\text{-}off}=489$ nm; FT-IR (KBr pellet): $\bar{\nu}/cm^{-1}=3350.7$ (N–H stretch), 2957.1, 2957.1 (aliphatic C-H stretch), 2858.8 (CH_2: C–H stretch), 1464.1, 1319.4 (NO_2 stretches); E. I. mass: $m/z=208$ (M^+), 151, 105; ^{1}H-NMR ($CDCl_3$, δ from TMS): 1.01 (t, 3H), 1.39–1.46 (m, 2H), 1.50–1.69 (m, 2H), 1.82–1.88 (m, 2H), 3.16–3.26 (q, 2H), 4.5 (broad, 1H), 6.54 (d, 2H), 8.09 (d, 2H); ^{13}C ($CDCl_3$, ppm): 13.85, 22.34, 28.34, 28.87, 29.12, 43.45, 110.92, 126.39, 153.50; elemental analysis (calculated for $C_{11}H_{16}N_2O_2$): %C = 63.12 (63.44), %H = 7.91 (7.74), %N = 13.14 (13.45).

***N*-Hexyl-4-nitroaniline (4).** Mp: 62–64 °C; UV–Vis (methanol): $\lambda_{max}=387$ nm, $\lambda_{cut\text{-}off}=480$ nm; FT-IR (KBr pellet): $\bar{\nu}/cm^{-1}=3348.7$ (N–H stretch), 2961.0, 2934.0 (aliphatic C–H stretch), 2856.8 (CH_2: C–H stretch), 1462.2, 1300.0 (NO_2 stretches); E. I. mass: $m/z=222$ (M^+), 151, 105; ^{1}H-NMR ($CDCl_3$, δ from TMS): 1.01 (t, 3H), 1.39–1.46 (m, 2H), 1.50–1.69 (m, 2H), 1.82–1.88 (m, 4H), 3.16–3.26 (q, 2H), 4.50 (broad, 1H), 6.54 (d, 2H), 8.09 (d, 2H); ^{13}C ($CDCl_3$, ppm): 13.88, 22.49, 26.62, 29.14, 30.77, 31.47, 43.48, 110.91, 126.39, 153.46; elemental analysis (calculated for $C_{12}H_{18}N_2O_2$): %C = 65.03 (64.84), %H = 8.37 (8.16), %N = 13.33 (12.89).

***N*-Heptyl-4-nitroaniline (5).** Mp: 62–64 °C; UV–Vis (methanol): $\lambda_{max}=387$ nm, $\lambda_{cut\text{-}off}=480$ nm; FT-IR (KBr pellet): $\bar{\nu}/cm^{-1}=3358.4$ (N–H stretch), 2967.0, 2930.1 (aliphatic C–H stretch), 2854.9 (CH_2: C–H stretch), 1464.1, 1300.0 (NO_2 stretches); E. I. mass: $m/z=236$ (M^+), 151, 105; ^{1}H-NMR ($CDCl_3$, δ from TMS): 0.99 (t, 3H), 1.39–1.46 (m, 6H), 1.50–1.69 (m, 2H), 1.82–1.88 (m, 2H), 3.16–3.26 (q, 2H), 4.50 (broad, 1H), 6.54 (d, 2H), 8.09 (d, 2H); ^{13}C ($CDCl_3$, ppm): 13.97, 22.53, 26.94, 28.95, 29.17, 31.70, 43.48, 110.92, 126.40, 153.48; elemental analysis (calculated for $C_{13}H_{20}N_2O_2$): %C = 65.85 (66.07), %H = 8.72 (8.53), %N = 12.45 (11.85).

***N*-Octyl-4-nitroaniline (6).** Mp: 52–54 °C; UV–Vis (methanol): $\lambda_{max}=387$ nm, $\lambda_{cut\text{-}off}=488$ nm; FT-IR (KBr pellet): $\bar{\nu}/cm^{-1}=3350.7$ (N–H stretch), 2967.2, 2922.4 (aliphatic C–H stretch), 2853.0 (CH_2: C–H stretch), 1464.1, 1300.0 (NO_2 stretches); E. I. mass: $m/z=250$ (M^+), 151, 105; ^{1}H-NMR ($CDCl_3$, δ from TMS): 0.99 (t, 3H), 1.39–1.46 (m, 8H), 1.50–1.69 (m, 2H), 1.82–1.87 (m, 2H), 3.16–3.36 (q, 2H), 4.50 (broad, 1H), 6.54 (d, 2H), 8.19 (d, 2H); ^{13}C ($CDCl_3$, ppm): 13.99, 22.58, 26.98, 27.75, 28.95, 29.17, 31.74, 43.48, 110.92, 126.39, 153.48; elemental analysis (calculated for $C_{14}H_{22}N_2O_2$): %C = 67.20 (67.17), %H = 9.02 (8.89), %N = 11.96 (11.92).

Powder SHG measurement

The powder SHG measurements were carried out using the Kurtz–Perry[28] method. The fundamental wavelength (1064 nm) of a Q-switched Nd:YAG laser (Continuum, Model 660B-10) was used. The detection system consisted of a monochromator (Jobin-Yvon, Model HRS-2) and oscilloscope (Tektronix, Model TDS 210, 60 MHz). Particle sizes of microcrystalline powder samples were graded using standard sieves; sizes ranging from 50–355 μm were studied. Urea was used for calibrating the powder SHG. The samples were loaded in glass capillaries having an inner diameter of 600 μm. The SHG emitted from the powder samples was collected by a concave mirror, collimated and focused onto the monochromator slit. The errors in the measured SHG's are typically about 10–15%. All the compounds showed very good stability under laser irradiation and no sign of decomposition, even on continued irradiation with a laser power of 1 GW cm^{-2} (6 ns, 10 Hz), was detected.

Crystal structure studies

X-Ray diffraction data were collected on an Enraf-Nonius MACH3 diffractometer. Mo-Kα radiation with a graphite crystal monochromator in the incident beam was used. Details of data collection, solution and refinement, anisotropic thermal parameters and full lists of bond lengths and angles are presented in the Supporting Information.

Results and discussion

Chen *et al.*[21] reported that **2** recrystallised from ether and ethanol–cyclohexane shows powder SHG intensities of 14 and 0.5 U respectively, whereas **1**, **3** and **4** are SHG inactive. They

Table 1 Powder SHG data for urea and **2** at various particle sizes

	SHG (arb. units)	
Particle size/μm	Urea	**2**
50–100	0.4	—
100–150	1.0	11.1
150–200	1.4	15.8
200–250	1.0	12.7
250–300	1.3	15.8
300–355	1.3	23.8
>355	1.0	19.8

did not study **5** but found that **6** recrystallised from ethanol–cyclohexane or ether showed a weak SHG of 0.05 U or no SHG activity respectively. Kurtz–Perry powder measurements we have carried out on **1**–**6** recrystallised from choloroform–toluene are in general agreement with these observations; **2** alone was found to be SHG active. The variation of SHG intensity of **2** with particle size is compared with that of urea in Table 1. The SHG of both urea and **2** are found to saturate above a particle size of ~150 μm indicating phase-matching behaviour. The average SHG of **2** at saturation is found to be about 17.6 U. Our investigation of a series of compounds, 7,7-bis(dialkylamino)-8,8-dicyanoquinodimethanes[26] has shown that the butyl, pentyl and hexyl derivatives are SHG active (11–19 U) whereas the derivatives with shorter (propyl) as well as longer (heptyl, octyl and dodecyl) alkyl chains are not. Crystal structure studies on these compounds showed that the alkyl chain length plays a crucial role in controlling the dipole orientations. When the alkyl chain is short as in the propyl derivative, the dipole–dipole interactions are dominant and result in a centrosymmetric crystal lattice. When the chain is long, a quasi-bilayer structure is formed with the dipoles forming a polar layer and the alkyl chains forming a nonpolar layer. Electrostatic interactions within and across the polar regions lead once again to a centrosymmetric crystal lattice. In the intermediate cases, the alkyl chain interactions interfere with the dipole–dipole interactions and lead to noncentrosymmetric crystal structures and appreciable SHG activity. The SHG capability in the pNA series confined to the butyl derivative alone also appears to be determined by the alkyl chain length effect.

The pNA derivatives **1**–**6** possess lower melting points than pNA indicating that the intermolecular interactions are weaker in their crystals compared to the parent system. This may be attributed partly to the reduction in the intermolecular H-bonding due to the replacement of one of the amino H atoms. More interestingly we find that these compounds exhibit a smooth progression of melting points to lower values as the chain length increases. This indicates that the alkyl chain exerts significant influence on the crystal packing. The high solubility of the alkylated pNA's caused some difficulty with their crystallisation. Exploration of a variety of solvents and solvent mixtures led to the choice of toluene–chloroform as a suitable solvent system to grow crystals of most of the compounds by slow evaporation. Since longer alkyl chain substituted compounds gave poor quality crystals, **1**, **2** and **3** were selected for detailed analysis.

1, **2** and **3** form yellow, transparent crystals. The crystallographic data for these three compounds are collected in Table 2. **1** belongs to the $P\bar{1}$ space group with two molecules in the asymmetric unit. The molecular structure is shown in Fig. 1 and the significant bond lengths and angles are collected in Table 3. Intermolecular H-bonds are observed in this crystal, connecting the nitro O atoms and amino H atoms ($r_{N_4\cdots O_{2'}}=3.012$ Å, $r_{N_{4'}\cdots O_{2''}}=3.007$ Å). These H-bonds connect the molecules into a polar zigzag chain extending approximately along the *b* axis (Fig. 2). Adjacent chains have opposite polarity and are related by the centre of inversion. **2** crystallises in the noncentrosymmetric space group $P2_12_12_1$ with two molecules in the asymmetric unit. The molecular structure is shown in Fig. 3 and the significant bond lengths and angles are collected in Table 4. This structure also showed intermolecular H-bonds ($r_{N_4\cdots O_{2''}}=3.081$ Å, $r_{N_{4'}\cdots O_2}=3.046$ Å) connecting molecules into zigzag chains running along the *b* axis (Fig. 4). However there are now pairs of chains running

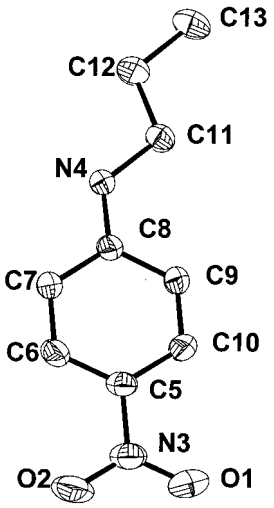

Fig. 1 Molecular structure of **1** from single crystal X-ray analysis; only one molecule in the asymmetric unit is shown; 25% probability thermal ellipsoids are indicated; H atoms are omitted for clarity.

Table 2 Crystallographic data for **1**, **2** and **3**

	1	**2**	**3**
Molecular formula	$C_9H_{12}N_2O_2$	$C_{10}H_{14}N_2O_2$	$C_{11}H_{16}N_2O_2$
Space group	Triclinic, $P\bar{1}$	Orthorhombic, $P2_12_12_1$	Monoclinic, $P2_1/c$
a/Å	5.076(2)	7.468(18)	6.192(3)
b/Å	13.123(16)	15.348(19)	15.61(7)
c/Å	15.190(5)	18.528(4)	11.851(6)
α/deg.	71.90(7)	90.0	90.0
β/deg.	81.91(4)	90.0	97.52(4)
γ/deg.	80.04(7)	90.0	90.0
V/Å^3	943.1(13)	2123(3)	1136(5)
Z	4	8	4
ρ/g cm^{-3}	1.269	1.215	1.218
μ/cm^{-1}	0.91	0.86	0.85
No. unique reflections	3311	3497	2725
No. of reflections	With $I>2\sigma_I$ 1873	With $I>2\sigma_I$ 1415	With $I>3\sigma_I$ 1593
No. of parameters	238	254	137
R (for $I>2\sigma_I$)	0.0405	0.0551	0.0460
wR^2	0.1564	0.1232	0.1338

Table 3 Significant (*a*) bond lengths and (*b*) angles in **1** from single crystal X-ray analysis (atom labelling is shown in Fig. 1)

(*a*) Atom–atom	Distance/Å	(*b*) Atom–atom–atom(–atom)	Angle/deg.
N(3)–O(1)	1.222(3)	O(1)–N(3)–O(2)	122.6(2)
N(3)–O(2)	1.233(3)	O(1)–N(3)–C(5)	118.9(2)
N(3)–C(5)	1.432(4)	O(2)–N(3)–C(5)	118.5(2)
N(4)–C(8)	1.340(3)	C(8)–N(4)–C(11)	124.6(2)
N(4)–C(11)	1.455(3)	C(10)–C(5)–C(6)	120.6(2)
C(5)–C(10)	1.376(3)	C(10)–C(5)–N(3)	120.0(2)
C(5)–C(6)	1.381(4)	C(6)–C(5)–N(3)	119.3(2)
C(6)–C(7)	1.360(4)	C(7)–C(6)–C(5)	119.7(2)
C(7)–C(8)	1.408(3)	C(6)–C(7)–C(8)	121.0(2)
C(8)–C(9)	1.369(4)	N(4)–C(8)–C(7)	119.9(2)
C(9)–C(10)	1.366(4)	N(4)–C(8)–C(9)	122.4(2)
		C(7)–C(8)–C(9)	117.8(2)
		C(10)–C(9)–C(8)	121.0(2)
		C(9)–C(10)–C(5)	119.9(2)
		N(4)–C(11)–C(12)	111.4(2)
		C(11)–C(12)–C(13)	113.3(3)
		O(1)–N(3)–C(5)–C(10)	−5.5(4)
		O(2)–N(3)–C(5)–C(6)	−6.4(4)
		C(11)–N(4)–C(8)–C(9)	−0.2(3)

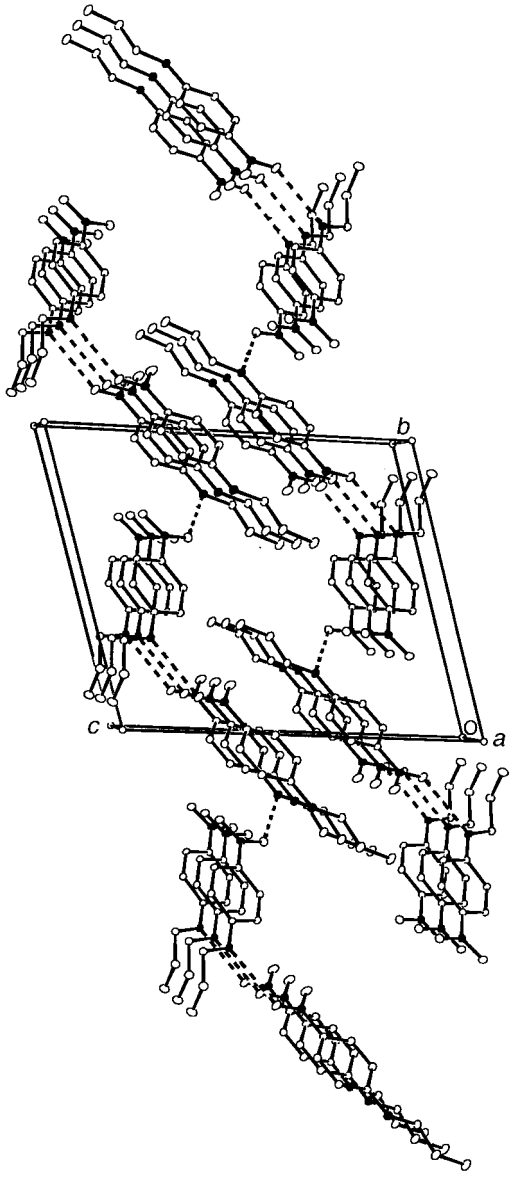

Fig. 2 Crystal packing in **1** viewed close to the *a* axis; H-bonds are shown as broken lines; N atoms are shown as filled circles.

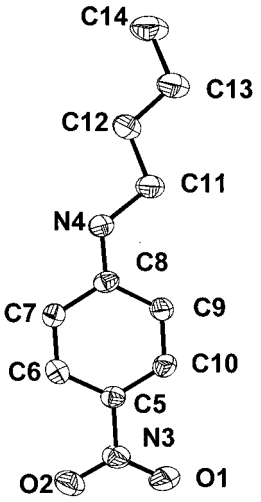

Fig. 3 Molecular structure of **2** from single crystal X-ray analysis; only one molecule in the asymmetric unit is shown; 25% probability thermal ellipsoids are indicated; H atoms are omitted for clarity.

together, the polarities within a pair being the same and the polarities of adjacent pairs directed opposite to each other. The chains within a pair are related by the screw rotation about the *b* axis whereas the chains in the adjacent pair are obtained by screw rotations about the *a* and *c* axes. Thus there is clearly no centre of inversion relating the polar chains oriented in opposite directions. Finally **3** is found to belong to the $P2_1/c$ space group with one molecule in the asymmetric unit. The molecular structure is shown in Fig. 5 and the significant bond lengths and angles are collected in Table 5. Intermolecular H-bonds ($r_{N4-O2'}=3.081$ Å) connect the molecules into chains as in **1** and **2**; a centre of inversion is formed as in the case of **1** (Fig. 6).

The crystal structures of **1**, **2** and **3** clearly illustrate the similarity in the packing motif and intermolecular interactions present in these alkylated pNA's. The singular behavior of **2** therefore appears to be a consequence of some subtle interactions. We have collected in Table 6 several structural parameters of the three crystals in an attempt to identify the critical features that lead to the observed dipole orientations and crystal packing. As noted earlier, all the three possess well-defined H-bonds. The values of $r_{H\text{-bond}}$ in Table 6 indicate that their strengths are quite comparable, but show a marginal decrease from **1** to **3**; this appears to be a consequence of the increasing alkyl chain length and contributes to the trend of decreasing melting points observed in the series. The closest

Table 4 Significant (*a*) bond lengths and (*b*) angles in **2** from single crystal X-ray analysis (atom labelling is shown in Fig. 3)

(*a*) Atom–atom	Distance/Å	(*b*) Atom–atom–atom(–atom)	Angle/deg.
O(1)–N(3)	1.201(4)	O(1)–N(3)–O(2)	122.3(3)
O(2)–N(3)	1.225(4)	O(1)–N(3)–C(5)	119.5(3)
N(3)–C(5)	1.443(5)	O(2)–N(3)–C(5)	118.2(3)
N(4)–C(8)	1.345(4)	C(8)–N(4)–C(11)	125.4(3)
N(4)–C(11)	1.434(5)	C(10)–C(5)–C(6)	120.9(3)
C(5)–C(10)	1.374(5)	C(10)–C(5)–N(3)	119.8(3)
C(5)–C(6)	1.384(5)	C(6)–C(5)–N(3)	119.2(3)
C(6)–C(7)	1.347(5)	C(7)–C(6)–C(5)	119.6(3)
C(7)–C(8)	1.416(5)	C(6)–C(7)–C(8)	120.9(3)
C(8)–C(9)	1.397(5)	N(4)–C(8)–C(9)	122.7(3)
C(9)–C(10)	1.357(5)	N(4)–C(8)–C(7)	118.0(3)
		C(9)–C(8)–C(7)	118.0(3)
		C(10)–C(9)–C(8)	120.7(3)
		C(9)–C(10)–C(5)	119.9(3)
		O(1)–N(3)–C(5)–C(10)	1.4(4)
		O(2)–N(3)–C(5)–C(6)	0.7(5)
		C(11)–N(4)–C(8)–C(7)	−176.5(4)

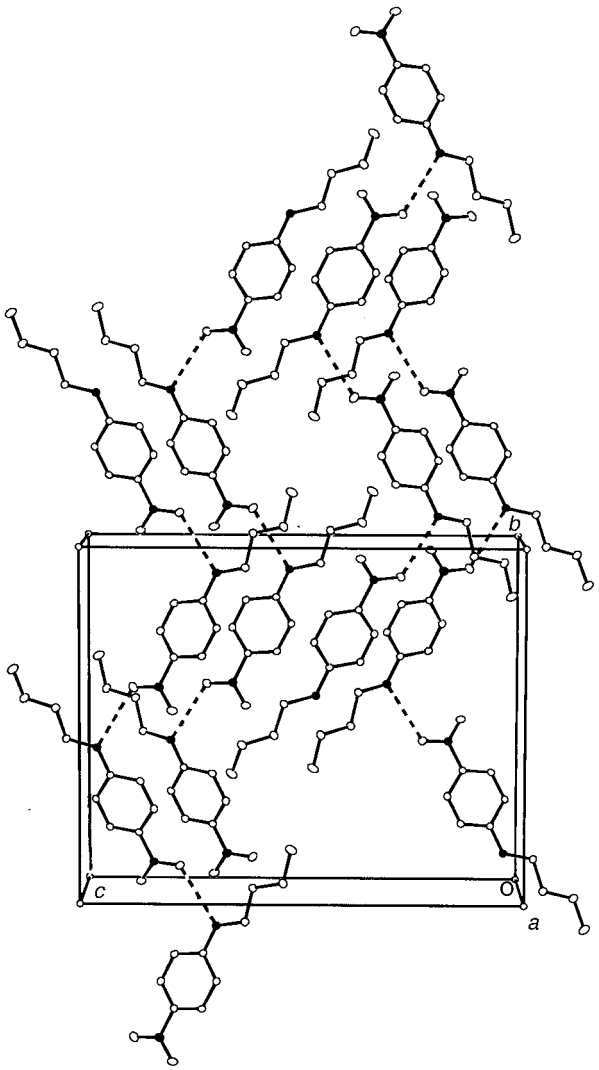

Fig. 4 Crystal packing in **2** viewed close to the *a* axis; H-bonds are shown as broken lines; N atoms are shown as filled circles.

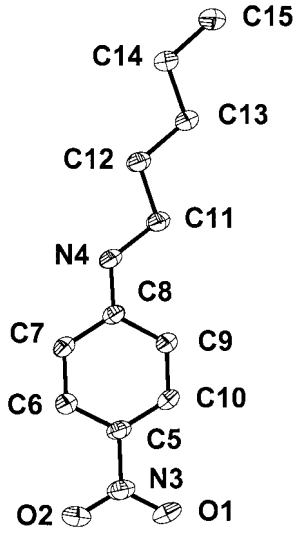

Fig. 5 Molecular structure of **3** from single crystal X-ray analysis; 25% probability thermal ellipsoids are indicated; H atoms are omitted for clarity.

C–C distance between alkyl chains of adjacent molecules, r_{C-C} shows an interesting trend. It decreases slightly from **1** to **2** and is considerably shorter in **3**. This indicates that the alkyl chain interactions set in with **3**, but are perhaps already incipient in **2**. The distance between the nitro N and amino N

Table 5 Significant (*a*) bond lengths and (*b*) angles in **3** from single crystal X-ray analysis (atom labelling is shown in Fig. 5)

(*a*) Atom–atom	Distance/Å	(*b*) Atom–atom–atom(–atom)	Angle/deg.
O(1)–N(3)	1.222(4)	O(1)–N(3)–O(2)	121.36(18)
O(2)–N(3)	1.2290(19)	O(1)–N(3)–C(5)	119.3(2)
N(3)–C(5)	1.436(6)	O(2)–N(3)–C(5)	118.75(19)
N(4)–C(8)	1.350(5)	C(8)–N(4)–C(11)	125.37(17)
N(4)–C(11)	1.440(2)	C(10)–C(5)–C(6)	120.9(2)
C(5)–C(10)	1.374(2)	C(10)–C(5)–N(3)	119.95(18)
C(5)–C(6)	1.386(4)	C(6)–C(5)–N(3)	119.1(2)
C(6)–C(7)	1.361(5)	C(7)–C(6)–C(5)	119.2(2)
C(7)–C(8)	1.397(2)	C(6)–C(7)–C(8)	121.36(18)
C(8)–C(9)	1.410(5)	N(4)–C(8)–C(7)	120.16(18)
C(9)–C(10)	1.367(5)	N(4)–C(8)–C(9)	121.6(2)
		C(7)–C(8)–C(9)	118.2(2)
		C(10)–C(9)–C(8)	120.0(2)
		C(9)–C(10)–C(5)	120.19(18)
		O(2)–N(3)–C(5)–C(10)	178.0(3)
		O(1)–N(3)–C(5)–C(6)	176.3(3)
		C(11)–N(4)–C(8)–C(7)	179.3(3)

atoms of the nearest oppositely aligned molecular dipoles, r_{dip} reflects the extent of dipole–dipole interaction. Based on the values of r_{dip} we infer that the electrostatic interaction decreases slightly from **1** to **2** but is enhanced in **3**. In the packing diagrams shown in Fig. 2, 4 and 6, it is seen that the alkyl

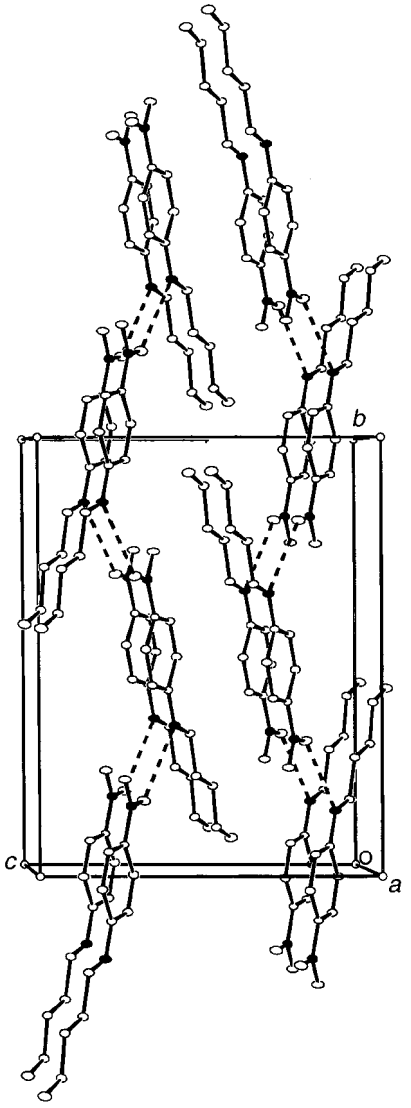

Fig. 6 Crystal packing in **3** viewed close to the *a* axis; H-bonds are shown as broken lines; N atoms are shown as filled circles.

Table 6 Structural parameters for **1**, **2** and **3** derived from single crystal X-ray analysis; $r_{H\text{-}bond}$: average of the H-bond distances; $r_{C\text{–}C}$: closest C–C distance between alkyl chains of adjacent molecules; r_{dip}: average distance between the nitro N and amino N of nearest oppositely aligned dipoles; $r_{C\text{–}ring}$: average of the closest distances between the end C of alkyl chain and benzene ring C atoms of adjacent molecules; θ: angle between the mean benzene planes of the nearest oppositely aligned molecules

Crystal	$r_{H\text{-}bond}$/Å	$r_{C\text{–}C}$/Å	r_{dip}/Å	$r_{C\text{-}ring}$/Å	θ/°
1	3.010	4.181	5.081	5.120	0.0
2	3.063	4.105	5.147	3.949	53.9
3	3.081	3.625	4.149	4.338	0.0

chain of one molecule gets close to the benzene ring of a near neighbour molecule leading to some van der Waals interaction. The proximity and hence the interaction may be quantified by taking an average of the distances between the end C atom of the alkyl chain and the C atoms of the benzene ring. This value, denoted as $r_{C\text{–}ring}$ shows that this chain–ring interaction is weak in **1**, slightly larger in **3** and very strong in **2**.

The observations listed above and their impact on the overall structures may be summarised as follows. In **1** the H-bonded chains are held together by moderate dipole–dipole electrostatic interactions. The chain length is short and there are no appreciable chain–chain or chain–ring interactions present. In **3** however, the longer alkyl chains interact strongly and bind the polar H-bonded molecular chains running in opposite directions; this facilitates stronger dipole–dipole interactions reflected in the low values of r_{dip}. The situations presented in **1** and **3** are conducive to the formation of centrosymmetric crystal lattices. In **2** the alkyl chains are still short so that strong chain–chain interactions do not set in, however they are long enough to collide with the benzene rings of nearby molecules. This leads to weaker dipole–dipole interactions compared to **1** and **3**. More significantly this interaction causes the benzene rings of adjacent oppositely aligned molecules to tilt away from the parallel disposition found in **1** and **3**; θ, the angle between the mean planes of the benzene rings is exactly zero in **1** and **3** and approximately 54° in **2** (Table 6). Though the major dipole components along the amino–nitro axis of the two molecules are still antiparallel in **2** (the angle between them is 179.5°), the dipole components orthogonal to it are no longer aligned antiparallel because of the tilt of the benzene planes. The situation is reminiscent of the symmetry breaking in crystals of urea.[29] The loss of the centre of inversion in **2** thus leads to the SHG capability; the SHG is moderate since the major β components cancel.

Structure analysis of the higher alkyl chain derivatives, **4**, **5** and **6** has been hampered by poor crystal quality. The longer alkyl chains in these molecules are probably disordered. Based on the SHG data and the structure of **3** described above, we assume that these systems have centrosymmetric crystal lattices.

Conclusion

The analysis of the crystal structures presented in this paper provides an explanation for the peculiar observation of SHG capability in the butyl derivative alone in the series of *N*-alkyl-*p*-nitroanilines. It clearly illustrates the critical role played by the alkyl chain length in developing the subtle interactions that lead to centrosymmetric or noncentrosymmetric crystal structures in the respective cases. It is observed that the dipole–dipole and H-bonding interactions are present in all the cases, but these interactions and their overall impact on the crystal structure are modulated by the alkyl chain interactions. This implies that the alkyl chains could be profitably used as crystal design elements in the fabrication of molecular materials for quadratic NLO applications. Molecules with large β tensor components perpendicular to the dipole axis will be of particular interest in this regard. We are currently exploring this idea.

Acknowledgements

Financial support from the Department of Science and Technology (Swarnajayanti Fellowship) and the use of the National Single Crystal Diffractometer Facility funded by the DST at the School of Chemistry, University of Hyderabad are gratefully acknowledged. PG thanks UGC for a Junior Research Fellowship.

Supporting information

Details of crystal structure analysis and listing of atomic coordinates, thermal parameters, bond distances and angles from X-ray crystal structure analysis for **1**, **2** and **3**.†

References

1 (*a*) D. S. Chemla and J. Zyss (eds.), *Nonlinear Optical Properties of Organic Molecules and Crystals*, Academic Press, New York, 1987, Vol. 1; (*b*) W. Nie, *Adv. Mater.*, 1993, **5**, 520; (*c*) D. R. Kanis, M. A. Ratner and T. J. Marks, *Chem. Rev.*, 1994, **94**, 195; (*d*) T. J. Marks and M. A. Ratner, *Angew. Chem., Int. Ed. Engl.*, 1995, **34**, 155; (*e*) N. J. Long, *Angew. Chem., Int. Ed. Engl.*, 1995, **34**, 21.

2 (*a*) G. R. Desiraju, *Crystal Engineering: The Design of Organic Solids*, Elsevier, Amsterdam, 1989; (*b*) M. C. Etter, *Acc. Chem. Res.*, 1990, **23**, 120; (*c*) J. A. Zerkowski, J. C. MacDonald and G. M. Whitesides, *Chem. Mater.*, 1994, **6**, 1250; (*d*) J. Bernstein, R. E. Davis, L. Shimoni and N. Chang, *Angew. Chem., Int. Ed. Engl.*, 1995, **34**, 1555; (*e*) G. R. Desiraju,. *Angew. Chem., Int. Ed. Engl.*, 1995, **34**, 2311; (*f*) V. A. Russell and M. D. Ward, *Chem. Mater.*, 1996, **8**, 1654.

3 (*a*) B. F. Levine, C. G. Bethea, C. D. Thurmond, R. T. Lynch and J. L. Bernstein, *J. Appl. Phys.*, 1979, **50**, 2523; (*b*) G. F. Lipscomb, A. F. Garito and R. S. Narang, *J. Chem. Phys.*, 1981, **75**, 1509; (*c*) J. Zyss, *J. Phys. D*, 1993, **26**, B198.

4 (*a*) J. Zyss, D. S. Chemla and J. F. Nicoud, *J. Chem. Phys*., 1981, **74**, 4800; (*b*) R. Twieg, A. Azema, K. Jain and Y. Y. Cheng, *Chem. Phys. Lett.*, 1982, **92**, 208; (*c*) M. Sigelle, J. Zyss and R. Hierle, *J. Noncryst. Solids*, 1982, **47**, 287.

5 (*a*) K. Rieckhoff and W. F. Peticolas, *Science*, 1965, **147**, 611; (*b*) D. F. Eaton, *Science*, 1991, **253**, 281; (*c*) T. Ukachi, T. Shigemoto and T. Sugiyama, *J. Opt. Soc. Am. B*, 1993, **10**, 1372.

6 (*a*) S. R. Marder, J. W. Perry and W. P. Schafer, *Science*, 1989, **245**, 626; (*b*) S. R. Marder, J. W. Perry and C. P. Yakymyshyn, *Chem. Mater.*, 1994, **6**, 1137.

7 M. D. Burland, D. R. Miller and A. C. Walsh, *Chem. Rev.*, 1994, **94**, 31.

8 (*a*) G. J. Ashwell, D. P. Jackson and W. A. Crossland, *Nature*, 1994, **368**, 438; (*b*) G. J. Ashwell, D. P. Jackson, G. Jefferies, R. I. Gentle and H. L. C. Kennard, *J. Mater. Chem.*, 1996, **6**, 137; (*c*) G. J. Ashwell, G. Jefferies, C. D. George, R. Ranjan, R. B. Charters and R. P. Tatam, *J. Mater. Chem.*,1996, **6**, 131; (*d*) D. K. Schwartz, *Surf. Sci. Rep.*, 1997, **27**, 241.

9 (*a*) I. Weissbuch, M. Lahav, L. Leiserowitz, G. R. Meredith and H. Vanherzeele, *Chem. Mater.*, 1989, **1**, 114; (*b*) V. Ramamurthy and D. F. Eaton, *Chem. Mater.*, 1994, **6**, 1128; (*c*) R. Hoss, O. Konig, V. Kramer-Hoss, U. Berger, P. Rogin and J. Hulliger, *Angew. Chem., Int. Ed. Engl.*, 1996, **35**, 1664.

10 (*a*) J. Zyss and L. Oudar, *Phys. Rev. A*, 1982, **26**, 2028; (*b*) J. Zyss and J.-F. Nicoud, *Curr. Opin. Solid State Mater. Sci.*, 1996, **1**, 533.

11 (*a*) K. N. Trueblood, E. Goldish and J. Donohue, *Acta Crystallogr.*, 1961, **14**, 1009; (*b*) J. L. Oudar and D. S. Chemla, *J. Chem. Phys.*, 1971, **66**, 2664; (*c*) C. C. Teng and A. F. Garito, *Phys. Rev. B*, 1983, **28**, 6766.

12 (*a*) P. D. Southgate and D. S. Hall, *Appl. Phys. Lett.*, 1971, **18**, 456; (*b*) P. D. Southgate and D. S. Hall, *J. Appl. Phys.*, 1972, **43**, 2765; (*c*) A. C. Skapski and J. L. Stevenson, *J. Chem. Soc., Perkin Trans. 2*, 1973, 1197; (*d*) A. Carenco, J. Jerphagnon and A. Periguad, *J. Chem. Phys.*, 1977, **66**, 3806; (*e*) G. Plough-

†CCDC reference number 1145/158. See http://www.rsc.org/suppdata/jm/1999/1699 for crystallographic files in .cif format.

Sorenson and E. K. Andersen, *Acta Crystallogr., Sect. C*, 1986, **42**, 1813.
13 G. F. Lipscomb, A. F. Garito and R. S. Narang, *Appl. Phys. Lett.*, 1981, **38**, 663.
14 (*a*) J. L. Oudar and R. Hierle, *J. Appl. Phys.*, 1977, **48**, 2699; (*b*) R. Twieg, A. Azema, K. Jain and Y. Y. Cheng, *Chem. Phys. Lett.*, 1982, **92**, 208.
15 J. Zyss, J.-F. Nicoud and M. Coquillay, *J. Chem. Phys.*, 1984, **81**, 4160.
16 M. S. Wong, V. Gramlich, C. Bosshard and P. Günter, *J. Mater. Chem.*, 1997, **7**, 2021.
17 D. S. Chemla and J. Zyss (eds.), *Nonlinear Optical Properties of Organic Molecules and Crystals*, Academic Press, New York, 1987, Vol. 2, p. 221.
18 H. Daigo, N. Okamoto and H. Fujimura, *Opt. Commun.*, 1988, **69**, 177.
19 S. D. Cox, T. E. Gier, G. D. Stucky and J. Bierlein, *J. Am. Chem. Soc.*, 1988, **110**, 2986.
20 M. Ogawa, M. Takahashi and K. Kuroda, *Chem. Mater.*, 1994, **6**, 715.
21 D. Chen, N. Okamoto and R. Matsushima, *Opt. Commun.*, 1989, **69**, 425.
22 T. W. Panunto, Z. Urbanczyk-Lipkowska, R. Johnson and M. C. Etter, *J. Am. Chem. Soc.*, 1987, **109**, 7786.
23 J. Maurin and T. M. Krygowski, *J. Mol. Struct.*, 1988, **172**, 413.
24 (*a*) T. C. W. Mak and J. Trotter, *Acta Crystallogr.*, 1965, **18**, 68; (*b*) B. L. Davydov, V. F. Zolin, L. G. Koreneva and M. A. Samokhina, *J. Appl. Spectrosc.*, 1973, **18**, 120.
25 (*a*) N. Okamoto, T. Abe, D. Chen, H. Fujimura and R. Matsushima, *Opt. Commun.*, 1990, **74**, 421; (*b*) R. Matsushima, K. Hiramatsu and N. Okamoto, *J. Mater. Chem.*, 1993, **3**, 1045; (*c*) M. Kato, M. Kiguchi, N. Sugita and Y. Taniguchi, *J. Phys. Chem.*, 1997, **101**, 8856.
26 P. Gangopadhyay, S. Sharma, A. J. Rao, D. N. Rao, S. Cohen, I. Agranat and T. P. Radhakrishnan, *Chem. Mater.*, 1999, **2**, 466.
27 (*a*) R. E. Parker, *Adv. Fluorine Chem.*, 1963, **3**, 63; (*b*) H. E. Smith, W. I. Cozart, T. de Paulis and F. M. Chen, *J. Am. Chem. Soc.*, 1979, **101**, 5186.
28 S. K. Kurtz and T. T. Perry, *J. Appl. Phys.*, 1968, **39**, 3798.
29 (*a*) P. Vaughan and J. Donohue, *Acta Crystallogr.*, 1952, **5**, 530; (*b*) J.-F. Nicoud and R. J. Twieg, in *Nonlinear Optical Properties of Organic Molecules and Crystals*, D. S. Chemla and J. Zyss (eds.), Academic Press, New York, 1987, Vol. 1, p. 257.

Paper 9/01591D